Supporting Information

Phosphine-Protected Atomically Precise Silver-Gold Alloy Nanoclusters and Their Luminescent Superstructures

Madhuri Jash,[†] Arijit Jana,[†] Ajay K. Poonia,[‡] Esma Khatun,[†] Papri Chakraborty,[†] Ankit Nagar,[†] Tripti Ahuja,[†] K. V. Adarsh*[,‡] and Thalappil Pradeep*[,†,§]

[†]DST Unit of Nanoscience (DST UNS) and Thematic Unit of Excellence (TUE), Department of Chemistry, Indian Institute of Technology Madras, Chennai 600036, India

[‡]Department of Physics, Indian Institute of Science Education and Research Bhopal, Bhopal 462066, India

[§]International Centre for Clean Water, IIT Madras Research Park, Chennai 600113, India

*E-mail: pradeep@iitm.ac.in, adarsh@iiserb.ac.in

Table of Contents

Instrumentation

UV-vis absorption spectroscopy

Perkin Elmer Lambda 25 UV-vis spectrometer was used to record the UV-vis spectra of nanoclusters. Absorption spectra were typically measured in the range of 200-1100 nm with a bandpass filter of 1 nm.

Photoluminescence (PL) spectroscopy

Photoluminescence measurement was carried out in a HORIBA, Jobin Yvon NanoLog fluorescence spectrometer with a bandpass of 3 nm for both emission and excitation spectra.

Dynamic light scattering (DLS)

DLS measurement was done using a Malvern Zetasizer ZSP instrument equipped with a 633 nm (He-Ne) laser.

Electrospray Ionization Mass Spectrometry (ESI MS)

The electrospray ionization mass spectra were measured in Waters Synapt G2Si High Definition Mass Spectrometer. This mass spectrometer consists of an electrospray source, quadrupole ion guide/trap, ion mobility cell, and TOF analyzer. Nitrogen gas was used as the nebulizer gas, and all the mass spectra were collected in positive ion mode. Mass spectrometric measurements were done by using the following conditions:
Flow rate: 30 µL/min, Capillary voltage: 3 kV, Cone voltage: 20 V, Source offset: 20 V, Source temperature: 100 °C, Desolvation temp: 150 °C, Desolvation gas flow: 400 L/h, Trap gas flow: 5 L/h.

Nuclear magnetic resonance (NMR) spectroscopy

Nuclear magnetic resonance spectroscopy measurements were carried out at room temperature by using a Bruker 500 MHz NMR spectrometer. Pure ligands (DPPB and DPPP) and the alloy nanoclusters were dissolved in $CDCl_3$ to collect ^{31}P NMR spectra.

X-ray photoelectron spectroscopy (XPS)

X-ray photoelectron spectroscopy (XPS) of alloy nanoclusters was performed by using an ESCA Probe TPD spectrometer of Omicron Nanotechnology. Monochromatic Al Kα (1486.69 eV) X-ray source was used. Samples were drop-casted on a sample stub, and measurements were carried out with constant analyzer energy of 50 eV for the survey scans and 20 eV for the specific regions. The binding energies in the spectra were calibrated with respect to the C 1s peak at 284.8 eV.

Field emission scanning electron microscopy (FESEM)

Scanning electron microscopy and energy dispersive X-ray spectroscopy analysis were performed with a Verios G4 UC, FEI instrument. Samples were prepared by drop-casting the

materials on a substrate (TEM grid was used for the good quality of pictures with good contrast) and drying them at room temperature. The sample was sputter coated with Au/Pd mixture to produce better-quality images without charging.

Transmission electron microscopy (TEM) and energy dispersive X-ray spectroscopy (EDS)

Transmission electron microscopy was performed using a JEOL 3010, 300 kV instrument at an accelerating voltage of 200 kV. The accelerating voltage was kept low to reduce beam-induced damage. Samples were prepared by drop casting the solution on a carbon-coated copper grid and dried under ambient conditions. EDS spectra were acquired using the attached Oxford Semistem system.

Hyperspectral microscopy (HSI)

Dark-field imaging of the cluster was performed using an Olympus BX-51 microscope and 100 W quartz halogen light source on a hyperspectral microscope, CytoViva Inc. A broadband white light was used for the optical imaging via a dark field condenser. A 100x oil immersion objective was used for collecting the scattered/emitted light from the nanocluster spheres. To prepare the sample, 2 µl of aggregates solution was drop-casted on a 1 mm thick ultrasonically cleaned glass slide and covered with a coverslip. Then it was sealed with nail polish on the sides to avoid drying of samples. In the overall procedure, care was taken such that only one side of the slide was exposed to chemicals. Imaging was done by a true-color charge-coupled device (CCD). A mercury lamp and appropriate filters (excitation and emission) were used for fluorescence images. Hyperspectral image analysis software was used for spectral analysis.

TCSPC measurements

To study the time-resolved PL lifetime of clusters and their aggregated states, we employed the HORIBA DeltaFlex time-correlated single photon count (TCSPC) spectrometer. The measurements were performed using the HORIBA DeltaDiode 405 nm laser. The obtained emission was collected using the HORIBA PPD-850 detector. The instrument response of the present setup is shown below.

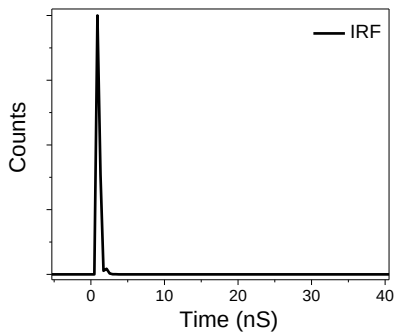

Figure. IRF of the TCSPC spectrometer.

Femtosecond pump-probe measurements

In our study, the excited state dynamics of samples are analyzed using ultrafast transient absorption spectroscopy. The setup consists of Spectra-Physics MaiTai oscillator, Spitfire Ti:sapphire optical amplifier to generate the 120 fs pulses centered at 800 nm. The output beams are passed through a second harmonic β-barium borate crystal to generate the 400 nm pulses, which are used to excite the samples (pump beam). The second harmonic pulses are separated from the fundamental beam with the help of a dichroic beam splitter. Then both 400 and residual 800 nm are sent to CDP ExciPro pump-probe spectrometer. Here the pump beam passes through a chopper, and a rotating neutral density filter controls the averaging and intensity of pulses. The 800 nm pulses are sent to a computer-controlled motion controller and a rotating CaF_2 crystal to produce time delayed white light continuum probe beam. Both pump and probe beam spatially overlapped on the sample, and then a change in absorbance of the probe beam was detected with the help of MS 2004 (600 lines/mm diffraction grating blazed at 600 nm) spectrometer and Si linear photodiode arrays. Then obtained data is chirp corrected to compensate for the group velocity dispersion.

PL spectra of 1 in methanol:

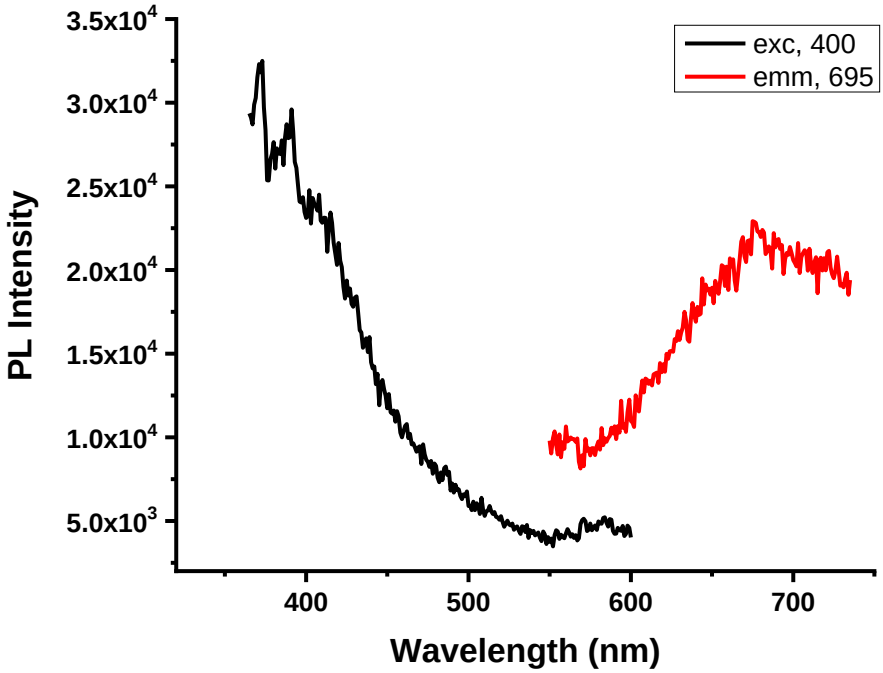

Figure S1. Excitation (black trace) and emission spectra (red trace) of **1** in methanol with large Stokes shift. The emission spectrum represents the very weakly emissive nature of the cluster, which is not visible to the naked eye.

Stability of 1 in the solid state:

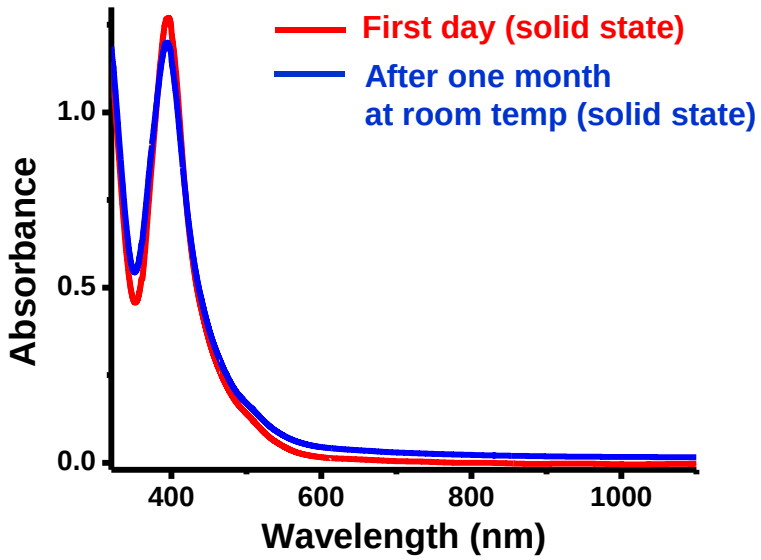

Figure S2. UV-vis spectrum of **1** in the solid state (red traces). The spectrum was also recorded after one month (blue trace) by storing the cluster film at room temperature and in the dark.

^{31}P NMR spectra of DPPB and 1:

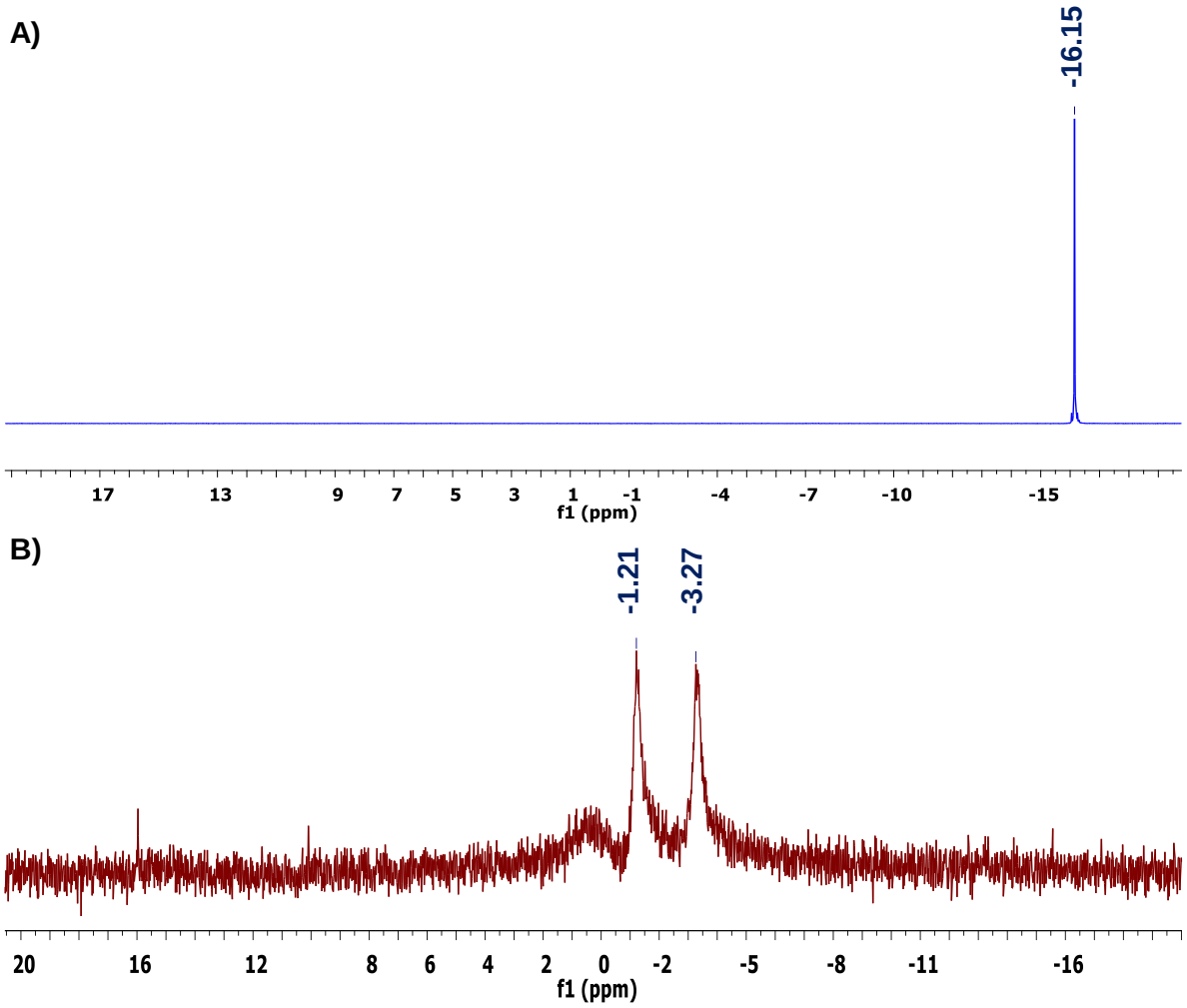

Figure S3. ^{31}P NMR spectra of (A) DPPB and (B) cluster **1**. The ^{31}P signal at -16.15 ppm for DPPB ligand disappears in **1** cluster due to the binding of ligands with the metal core, confirmed by the appearance of two new broad peaks at -3.27 and -1.21 ppm in the nanocluster.

XPS spectra of 1:

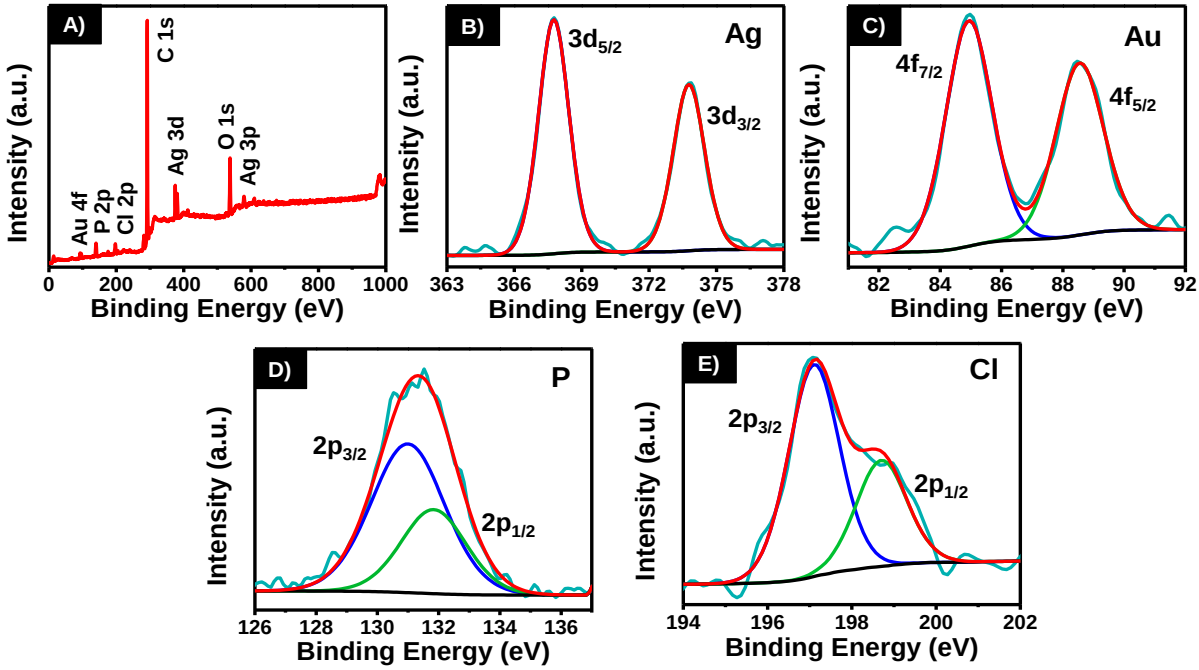

Figure S4. (A) XPS survey spectrum of **1** shows all the expected elements. (B) The Ag 3d region. Ag $3d_{5/2}$ appeared at 367.8 eV. (C) The Au 4f region. Au $4f_{7/2}$ appeared at 85.4 eV. (D) The P 2p region. P $2p_{3/2}$ appears at 131.8 eV. (E) The Cl 2p region. Cl $2p_{3/2}$ appears at 197.9 eV. P and Cl positions confirm their binding with the nanocluster.

TEM EDS of 1:

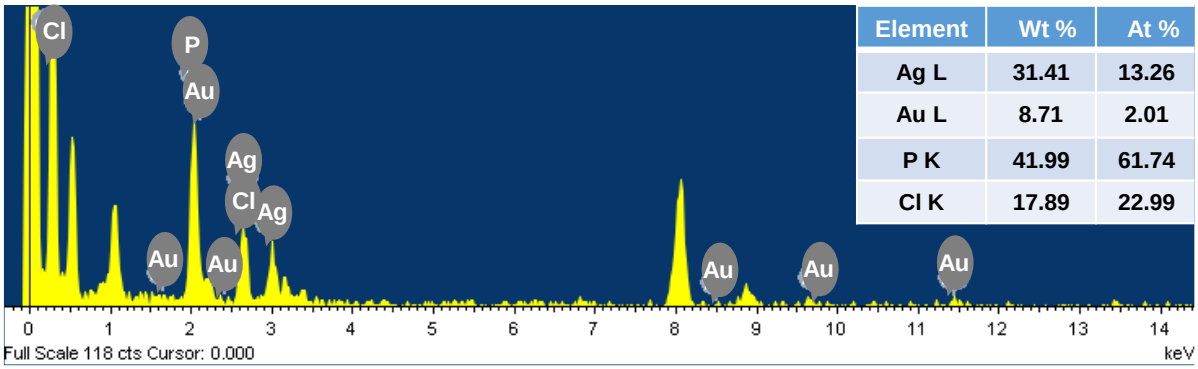

Element	Wt %	At %
Ag L	31.41	13.26
Au L	8.71	2.01
P K	41.99	61.74
Cl K	17.89	22.99

Figure S5. TEM EDS of **1** with quantification of the respective elements.

UV-vis spectra of 1 in the aggregated state:

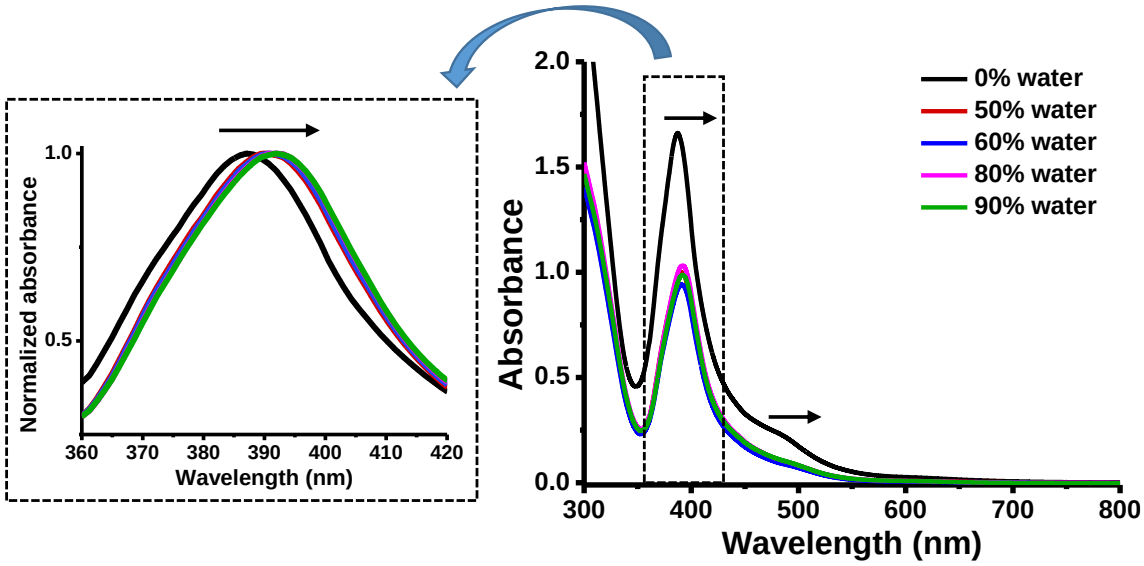

Figure S6. UV-vis spectra of **1** in methanol/water mixtures with different fractions of water. Here the cluster concentration was 1 mg/mL.

Table S1. Average lifetime of **1** in different states

Sample	**τ_1 (ns) (A_1)**	**τ_2 (ns)(A_2)**	**τ_3 (ns)(A_3)**	**τ_{avg}(ns)**
f_w 0%	1.56±0.02 (51)	19.36±0.22 (34)	130.31±1.08 (15)	26.8
f_w 70%	5.82±0.12 (47)	60.35±1.02 (32)	498.70±6.78 (22)	131.8
Film	0.56±0.03 (52)	86.8±3.67 (13)	856.75±19.54 (35)	311.4

PL spectra of aggregates of 1 after oxygen exposure:

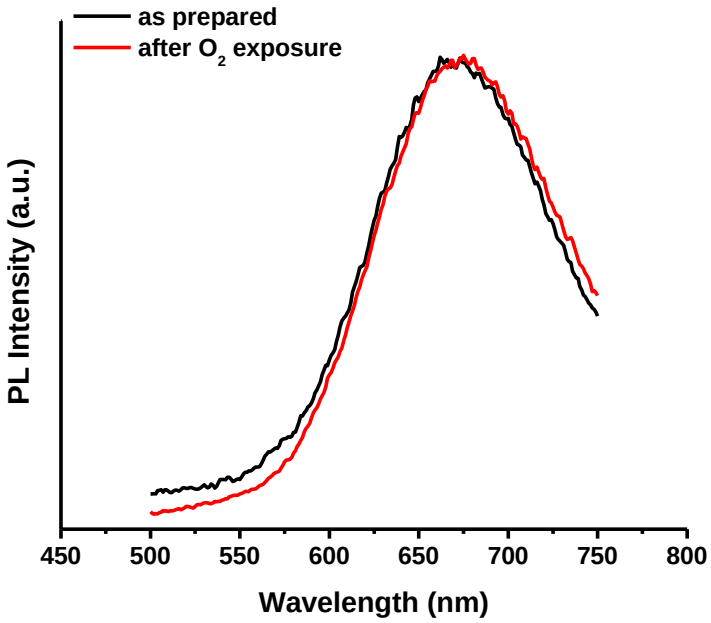

Figure S7. PL spectra of cluster **1** in methanol/water mixtures before (black) and after (red) exposure to O_2, which does not show any luminescence change.

TEM images of the hollow spheres:

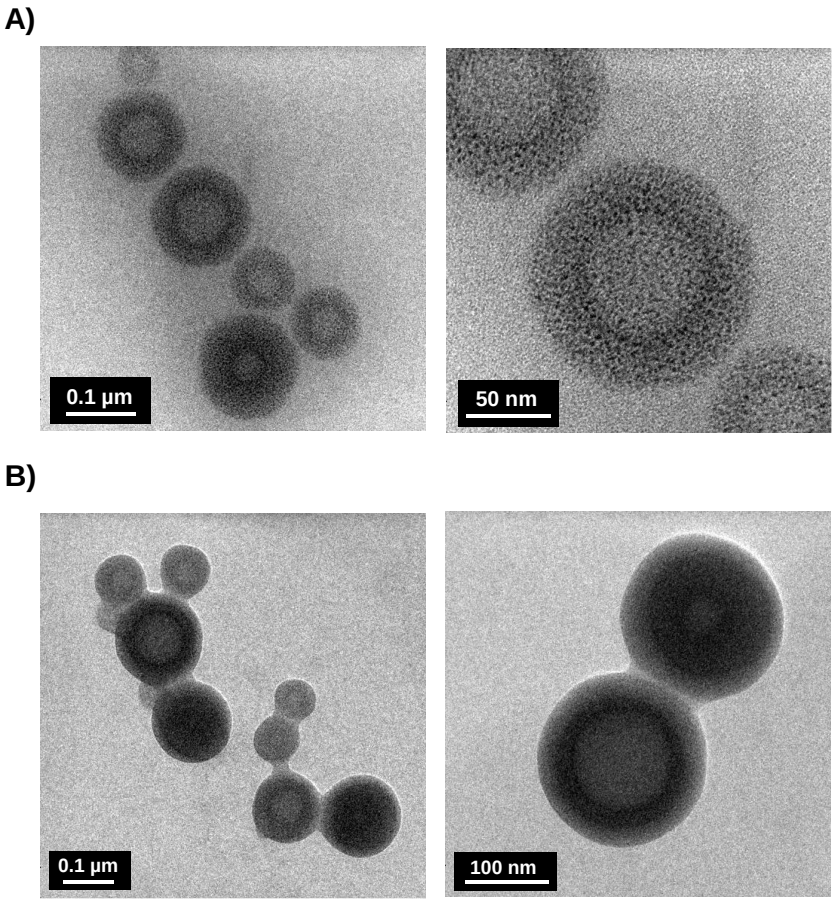

Figure S8. (A) TEM images of the hollow spheres with different magnifications. (B)TEM images presenting the assembly of more than one superstructure.

Stability of superstructures:

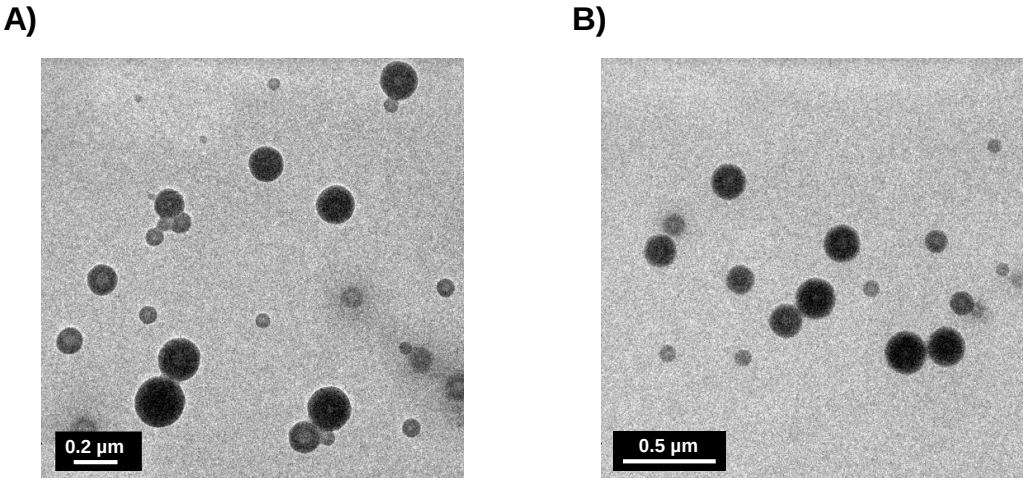

Figure S9. TEM images were collected after one week of the formation of aggregates of **1** for f_w 70%. (A) The liquid sample was drop-casted after one week, and (B) the drop-casted sample was kept for one week to check its stability.

Optical properties of 2:

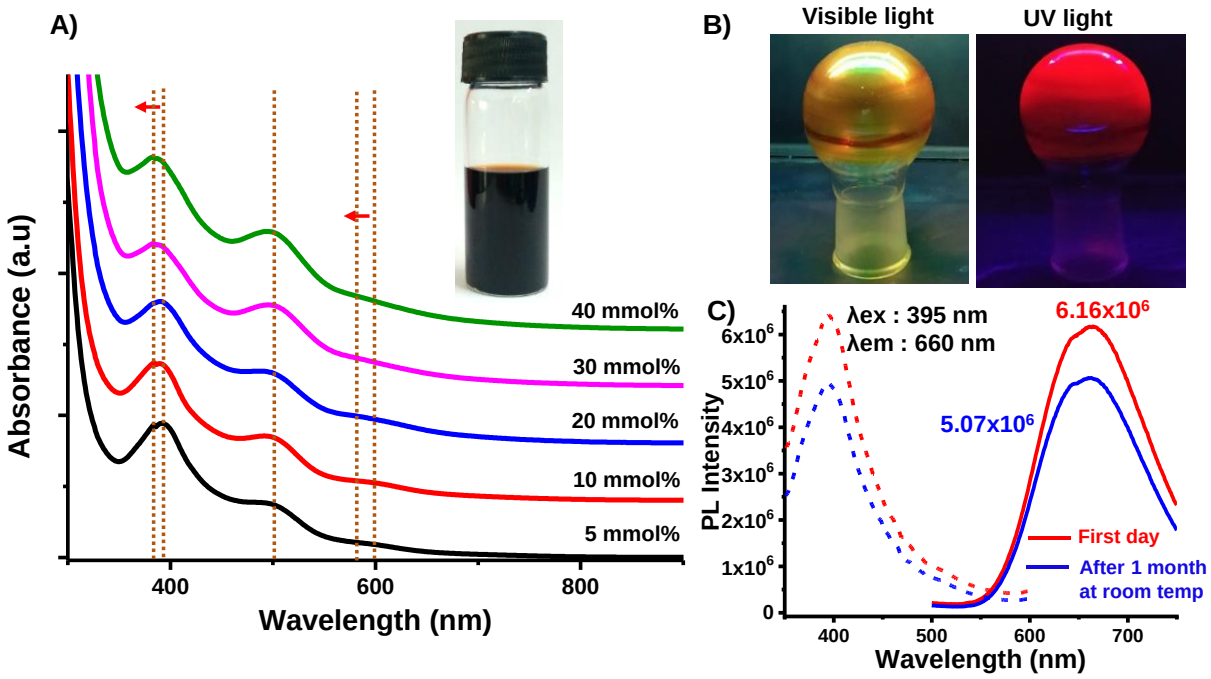

Figure S10. (A) UV-vis absorption spectra of $Ag_{15-x}Au_x$ by varying the amount of doped gold from 5 mmol % to 40 mmol %. Inset: Photograph of the cluster in methanol under visible light. (B) Photograph of the solid-state cluster **2** (vacuum dried) under visible and UV light, respectively. (C) Excitation (dotted line) and emission spectra (solid line) of **2** in the solid state were collected on the first day and after storing the sample at room temperature for a month.

PL spectra of 2 in methanol:

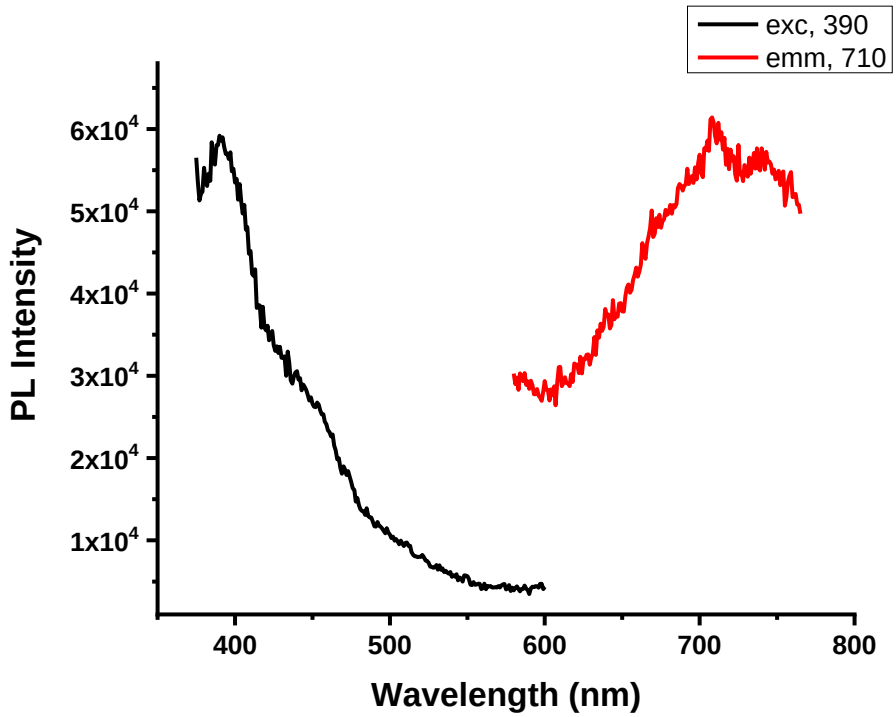

Figure S11. Excitation (black trace) and emission spectra (red trace) of **2** in methanol with large Stokes shift. The emission spectrum represents the weakly emissive nature of the cluster, which is not visible to the naked eye.

Stability of 2 in the solid state:

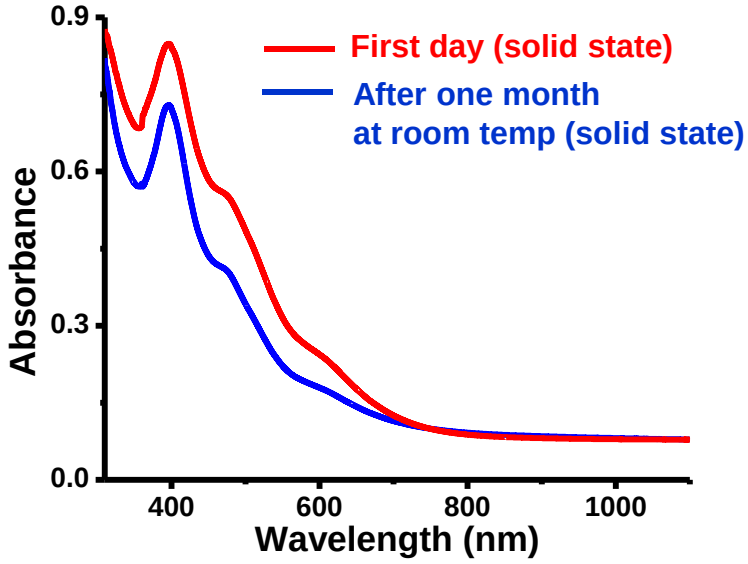

Figure S12. UV-vis spectrum of **2** in the solid state (red traces). The spectrum was also recorded after one month (blue trace) by storing the cluster film at room temperature and in the dark.

^{31}P NMR spectra of DPPP and 2:

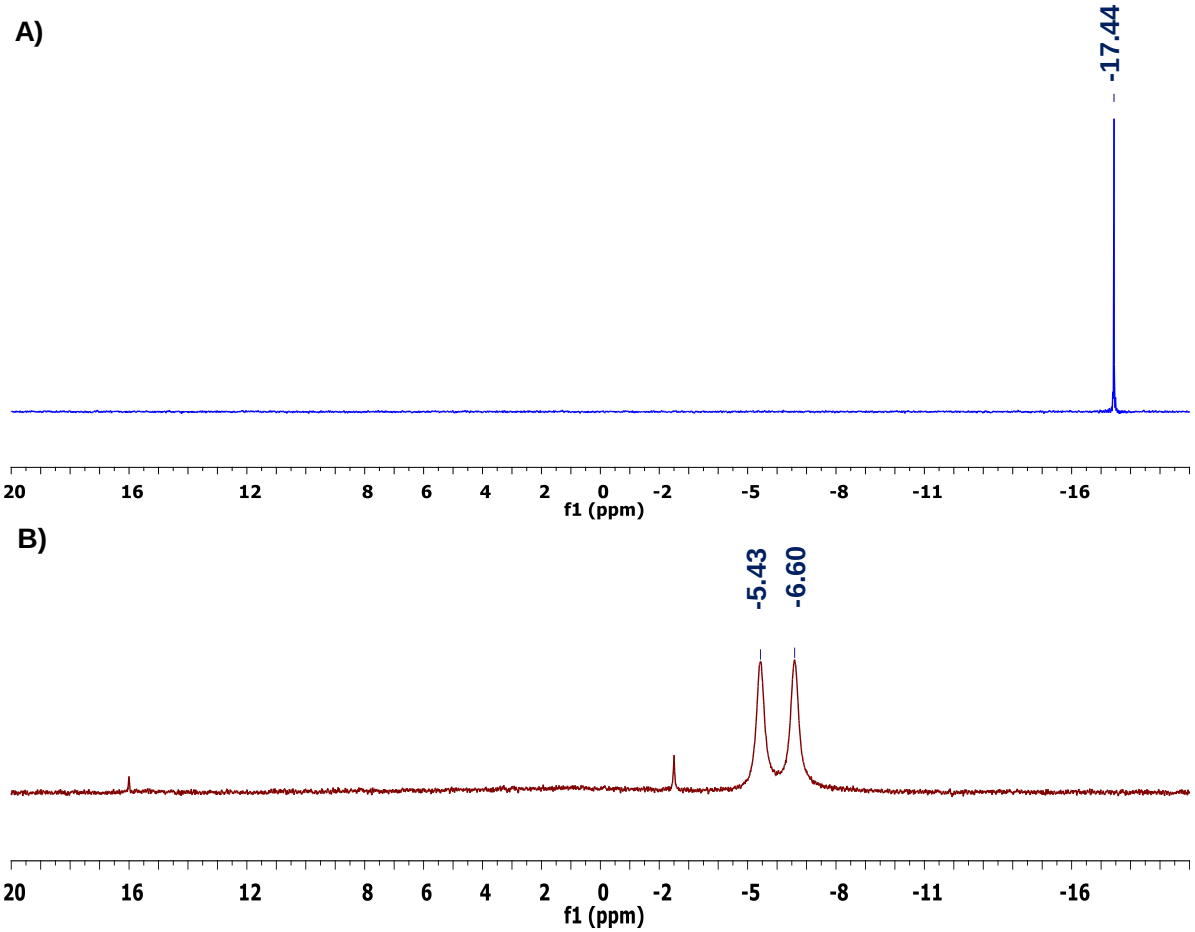

Figure S13. ^{31}P NMR spectra of (A) DPPP and (B) cluster **2**. The ^{31}P signal at -17.44 ppm for DPPP ligand disappears in **2** due to the binding of ligands with the metal core, which is also confirmed by the appearance of two new broad peaks at -6.60 and -5.43 ppm in the nanoclusters.

XPS spectra of 2:

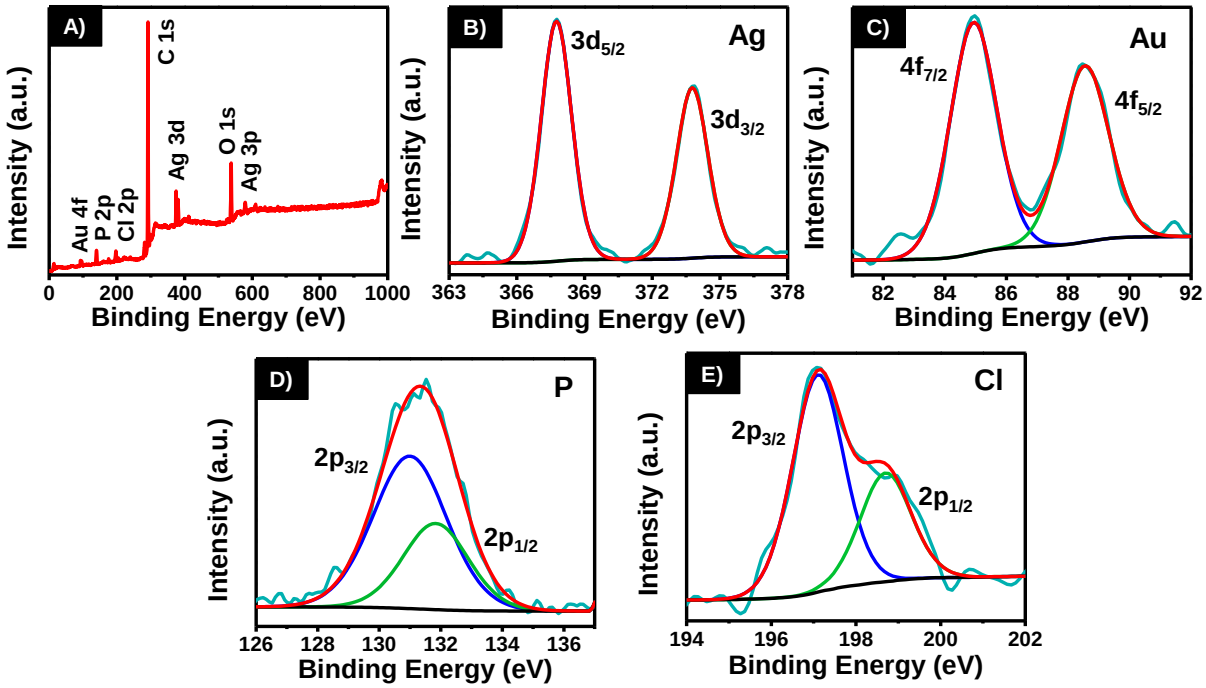

Figure S14. (A) XPS survey spectrum of **2** shows all the expected elements. (B) The Ag 3d region. Ag $3d_{5/2}$ appeared at 367.7 eV. (C) The Au 4f region. Au $4f_{7/2}$ appeared at 84.9 eV. (D) The P 2p region. P $2p_{3/2}$ appears at 130.9 eV. (E) The Cl 2p region. Cl $2p_{3/2}$ appears at 197.1 eV. The binding energies of P and Cl confirm their binding with the nanocluster.

TEM EDS of 2:

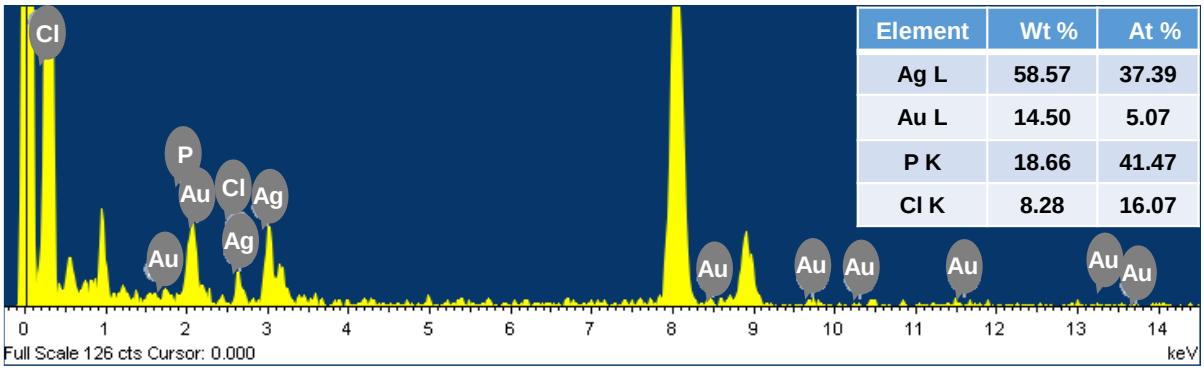

Element	Wt %	At %
Ag L	58.57	37.39
Au L	14.50	5.07
P K	18.66	41.47
Cl K	8.28	16.07

Figure S15. TEM EDS of **2** with quantification of the respective elements.

UV-vis spectra of 2 in the aggregated state:

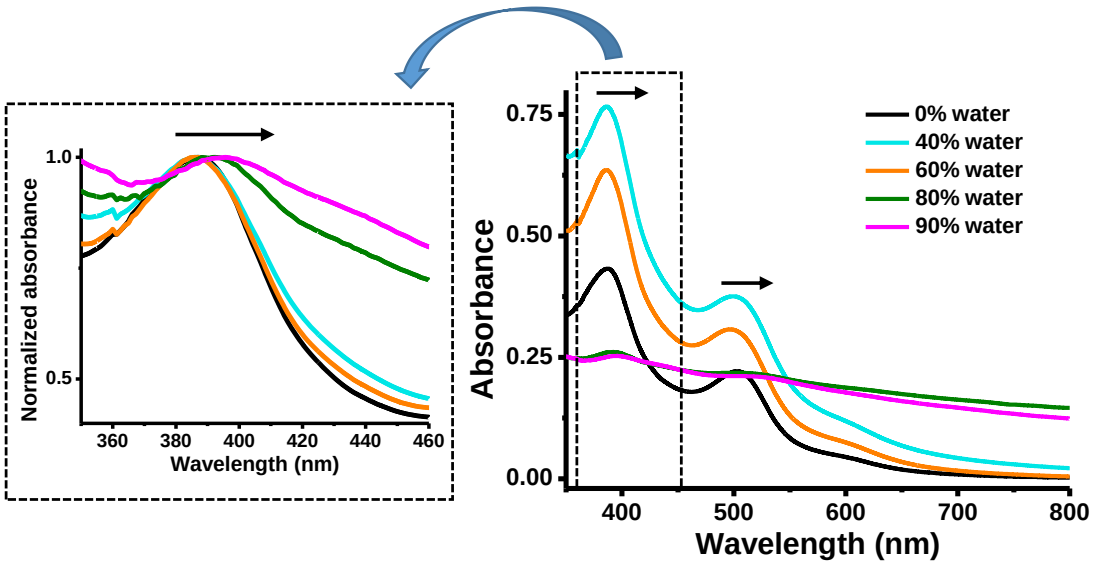

Figure S16. UV-vis spectra of **2** in methanol/water mixtures with different fractions of water. For f_w 80% and 90%, the baseline of the UV-vis spectra went high due to the formation of bigger size particles. For all cases, the cluster concentration was 1 mg/mL.

Lifetime measurements of 2 and its aggregates:

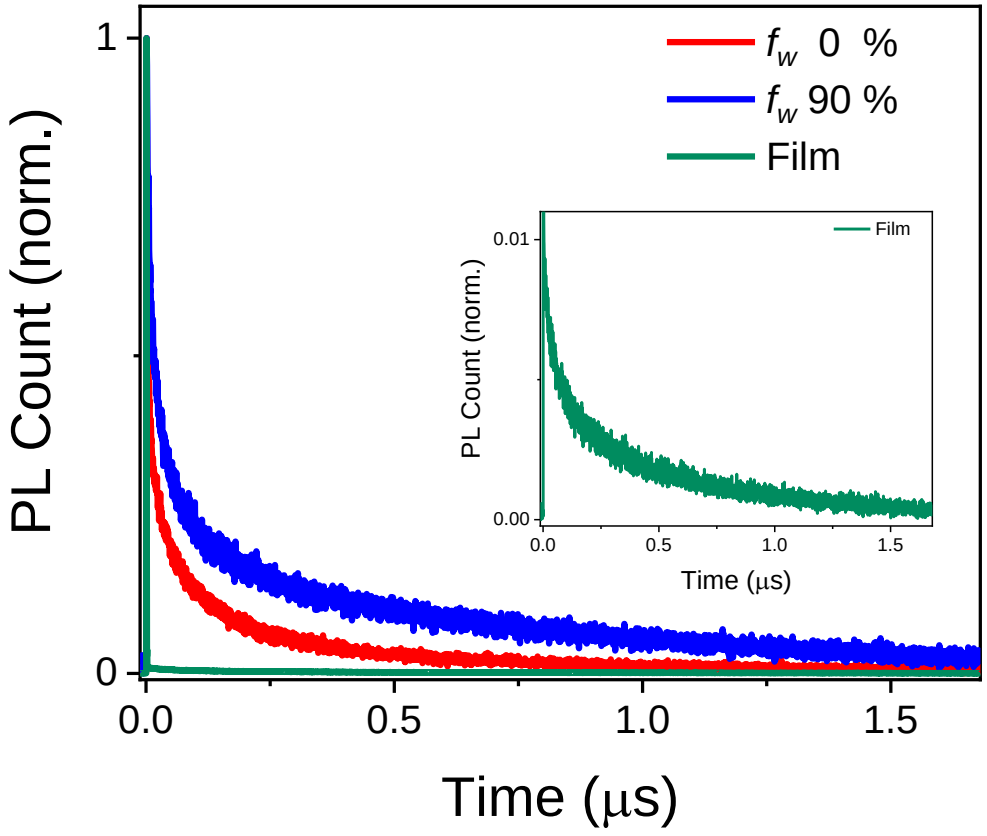

Figure S17. PL decay curves measured by TCSPC for f_w 0%, 90%, and film of cluster **2**.

Table S2. Average lifetime of **2** in different states

Sample	**τ_1 (ns) (A_1)**	**τ_2 (ns)(A_2)**	**τ_3 (ns)(A_3)**	**τ_{avg}(ns)**
0%	1.77±0.03 (55)	35.39±0.49 (28)	252.99±2.50 (17)	53.9
70%	6.57±0.18 (44)	51.50±1.06 (34)	607.20±10.46 (22)	153.9

PL spectra of aggregates of 2 after oxygen exposure:

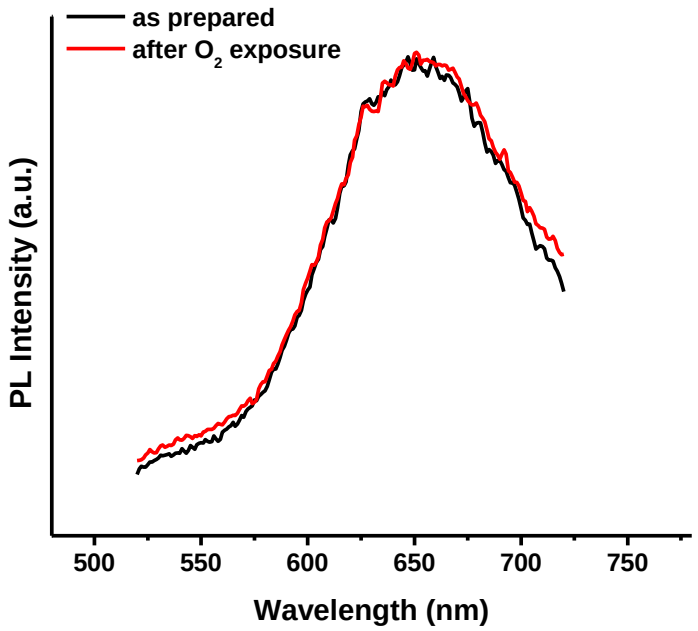

Figure S18. PL spectra of cluster **2** in methanol/water mixtures before (black) and after (red) exposure to O_2, which does not show any luminescence change.

DLS measurements of aggregates of 2:

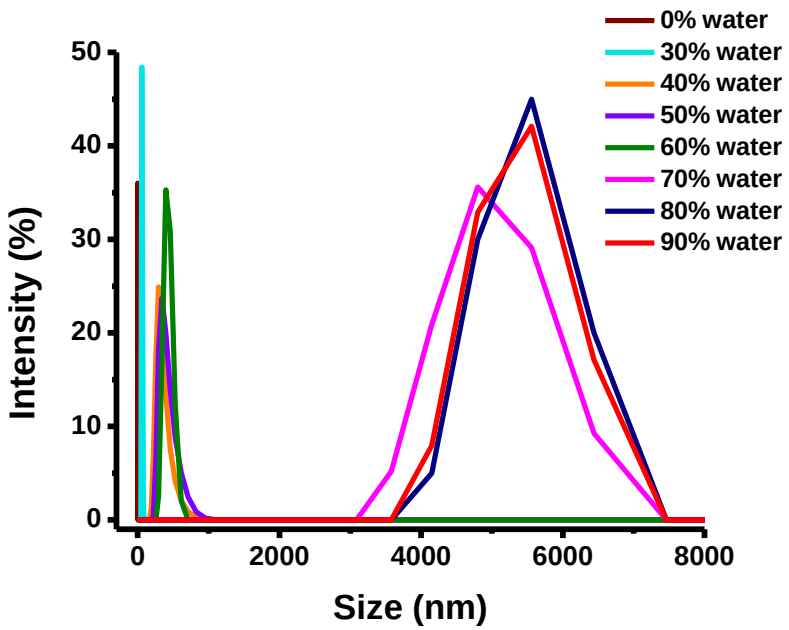

Figure S19. DLS spectra of **2** in methanol/water mixtures with different fractions of water. For all cases, the cluster concentration was 1 mg/mL.

Microscopic characterization of aggregates of 2:

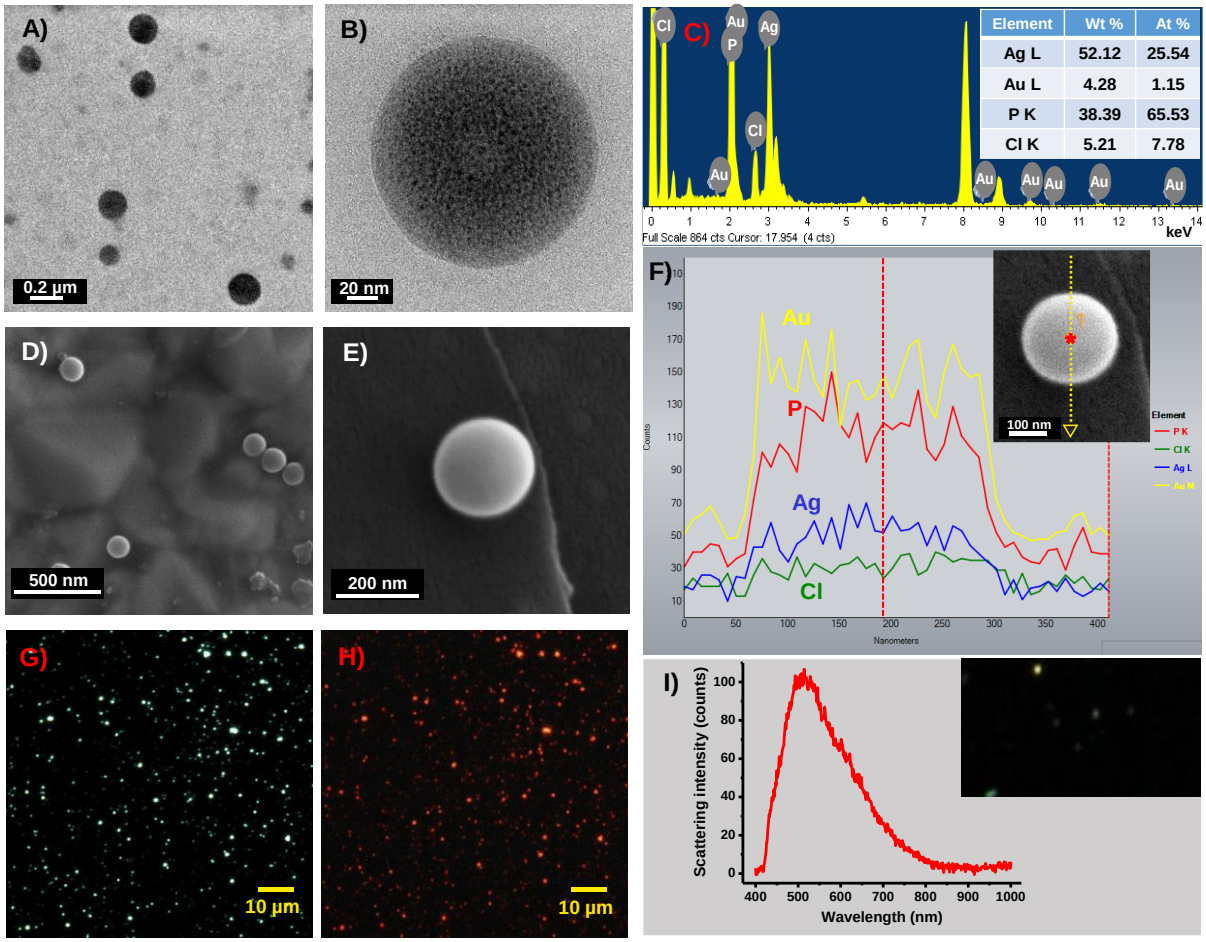

Figure S20. Microscopic characterization of the aggregates of **2** formed in f_w 70%. (A) and (B) are the TEM images of the spheres with different magnifications. (C) TEM EDS and elemental composition of the aggregates. (D) and (E) are the FESEM images with different magnifications. (F) SEM EDS line scans were measured along a single sphere indicated by the arrow. (G) Dark field image and (H) fluorescence image of the cluster aggregates immobilized on an ultra-clean glass slide. (I) Average scattering spectrum of the aggregates.

TA pump-probe spectra of 2 in different states:

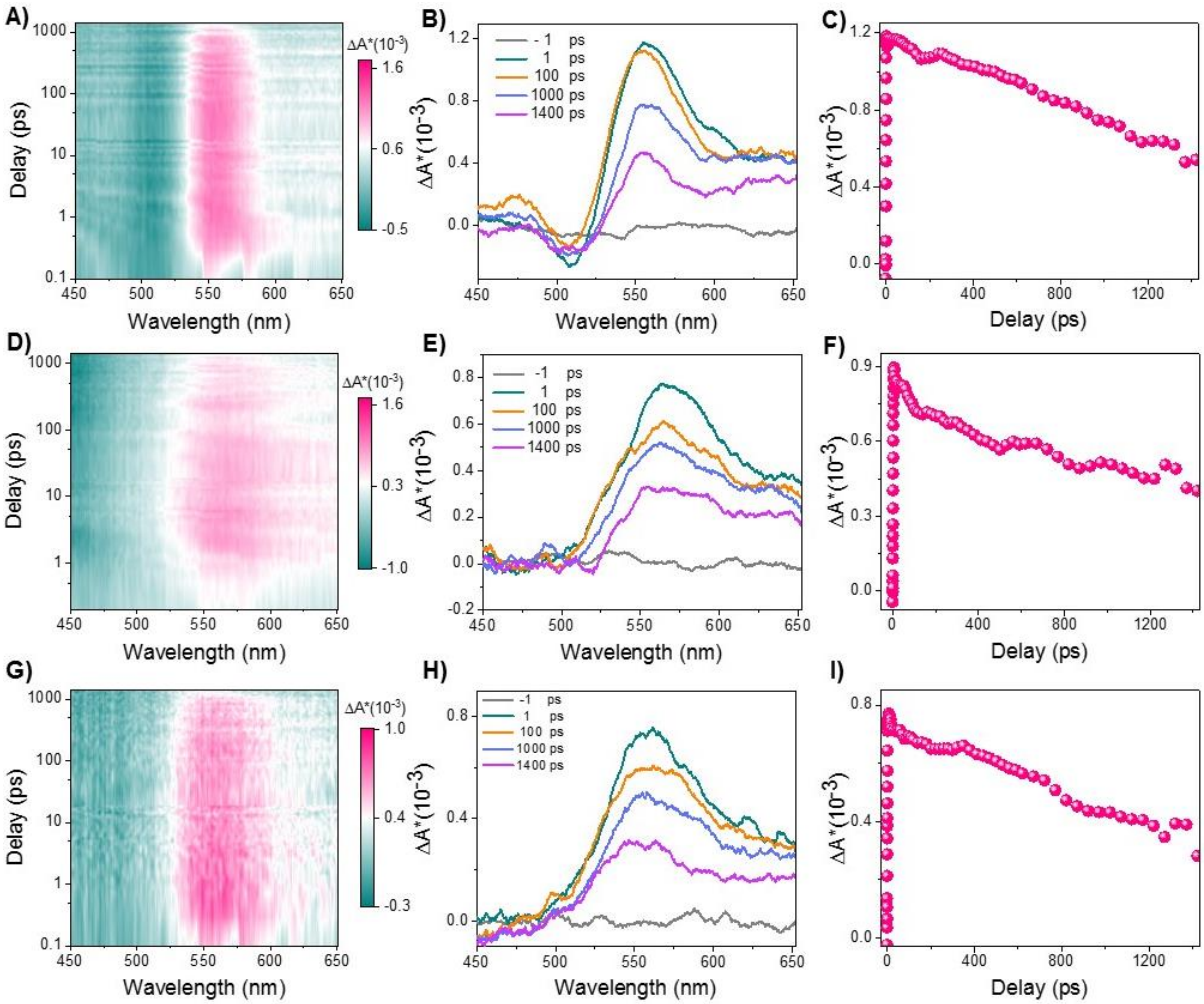

Figure S21. The fs-TA pump-probe spectra of 2. (A) Contour plot, (B) TA spectral profile as a function of time delay, and (C) transient kinetic traces at selected wavelength 555 nm peak measured for **2** in methanol. The same measurements have also been done for the aggregates formed in f_w 70% (D-F) and in the solid state (G-I).

Stability of Ag-Au alloy clusters at 4 °C:

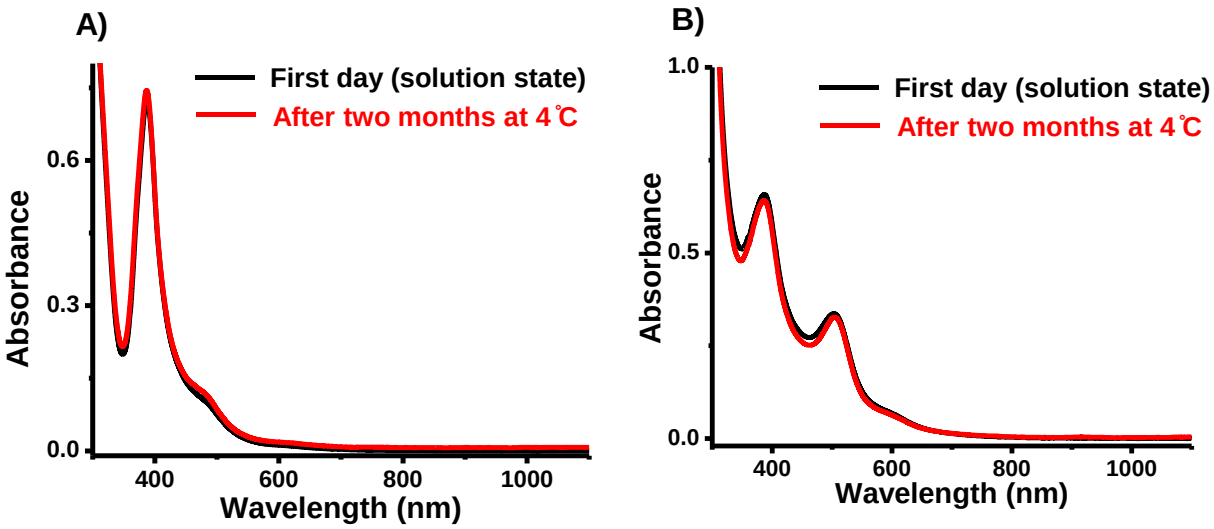

Figure S22. UV-vis spectra of (A) **1** and (B) **2** (black traces) in methanol. For both cases, the spectra were again recorded after two months (red trace) by dissolving the solid clusters stored at 4 °C.